ISSN: 2688-8645

An Epitaxial Layer Thickness Inversion Framework Based on Cauchy Dispersion and Multiple-Beam Interference Models

Zihan Xue *

Liaoning Technical University, Huludao, Liaoning, China

* Corresponding author Email: xuezihan_2023@163.com

Abstract

For measuring the thickness of epitaxial layers under infrared reflectance spectroscopy conditions, this paper proposes a thickness inversion method that integrates spectral preprocessing, interferometric model identification, and iterative optimization of dispersion parameters. First, the Savitzky–Golay filter is applied to suppress high-frequency noise while preserving the extrema characteristics of the interference fringes. Based on this, a dual-beam interference thickness calculation model is established, and the Cauchy dispersion model is introduced to describe the variation of refractive index with wavelength. Nonlinear least squares and damped iteration are then used to achieve a simultaneous estimation of the refractive index parameters and thickness. Furthermore, by combining interface reflectance and coherence length criteria to identify multi-beam interference conditions, a corresponding thickness correction model was established to mitigate the impact of higher-order reflections on the inversion results. Experimental results show that, after correction for multi-beam interference, the thicknesses obtained under 10° and 15° incidence conditions are 8.463 μm and 8.532 μm, respectively, demonstrating good consistency. This method can adapt to different incidence conditions and material dispersion characteristics, providing a highly versatile computational approach for measuring the thickness of thin films and epitaxial layers based on infrared interferometric spectroscopy.

Keywords

Epitaxial Layer Thickness Inversion; Cauchy Dispersion Model; Multiple-Beam Interference Model.

1. Introduction

The thickness of thin films and epitaxial layers is a critical parameter in material preparation and the characterization of optical properties; achieving accurate and stable thickness inversion using non-contact measurement data is of great significance [1][2]. Infrared reflectance spectroscopy can reveal changes in the optical path length within a material through interference fringes, providing a basis for thickness calculation. However, factors such as spectral noise, refractive index dispersion, and multiple reflections at interfaces in actual measurements complicate the relationship between interference features and thickness. Traditional methods often rely on a fixed refractive index or a single dual-beam interference model, which can lead to model deviations under broad-spectrum and multi-reflection conditions, thereby affecting the consistency of results across different measurement conditions [3].

To address these issues, this paper proposes a framework for an infrared interferometric thickness inversion algorithm. This framework combines a two-beam interference model with the Cauchy dispersion model, using nonlinear least squares and damped iteration to achieve the simultaneous update of refractive index parameters and thickness. Additionally, it identifies

ISSN: 2688-8645

interference modes based on interfacial reflectance and coherence length, and introduces a multi-beam interference model for correction when higher-order reflections cannot be neglected. The main innovation of this paper lies in integrating dispersion modeling, parameter iteration, and interference mode identification into a unified framework, thereby enhancing the model's adaptability to different optical conditions. The effectiveness of this method is validated using infrared reflectance spectra of epitaxial layers measured at different incident angles.

2. Infrared Spectral Data Preprocessing and Feature Enhancement

The experimental data consist of four sets of infrared reflectance spectra, mainly containing two variables: wavenumber and reflectance. Two sets were obtained from silicon carbide wafers, while the other two were obtained from silicon wafers, measured at incidence angles of 10° and 15°, respectively. All spectral datasets use the same wavenumber range, from 399.67 to 4000.122 cm^{-1}. Subsequent calculations are performed directly on the wavenumber–reflectance sequences. Extremum information is extracted from the periodic oscillation characteristics of the spectra and is then used for epitaxial layer thickness inversion.

2.1. Savitzky–Golay Filtering

The measured infrared reflectance spectra contain a certain amount of high-frequency noise. These local fluctuations may affect the localization of extrema and further increase the uncertainty in thickness calculation. To reduce the influence of noise while preserving the peak positions, peak shapes, and overall variation trend of the interference fringes as much as possible, Savitzky–Golay filtering is applied to smooth the original spectra [4].

Savitzky–Golay filtering performs a low-order polynomial least-squares fit to local data within a sliding window and replaces the original observation at the center of the window with the fitted value. Compared with a simple moving average, this method causes less shift in peak positions and is therefore more suitable for infrared spectral data with periodic oscillation characteristics.

The filtered reflectance can be expressed as:

$$R_{\mathrm{smooth}}(i)=\sum_{j=-k}^{k} c_j R(i+j) \tag{1}$$

where $R(i)$ is the original reflectance at the ith sampling point, c_j is the filtering coefficient, and k is the half-window width. The filtering coefficients are determined through least-squares fitting of a local polynomial, with the optimization form given by:

$$\min_{\mathbf{c}} \sum_i \left[R(i)-\sum_{m=0}^{M} c_m i^m \right]^2 \tag{2}$$

where M denotes the order of the local fitting polynomial. Based on the actual smoothing performance of the spectra and the preservation of peak shapes, the polynomial order is finally set to $M=3$, and the window length is set to $W=15$, satisfying $W=2k+1$. This parameter combination can suppress local random fluctuations while avoiding the loss of interference extrema caused by excessive smoothing.

2.2. Data Preprocessing Results

Figure 1 shows the spectral data before and after preprocessing. After Savitzky–Golay filtering, the local high-frequency fluctuations in the original spectra are clearly reduced, while the overall periodic structure of the interference fringes and the main peak and valley positions remain nearly unchanged. The filtering therefore does not noticeably alter the main spectral features used in the subsequent thickness calculation.

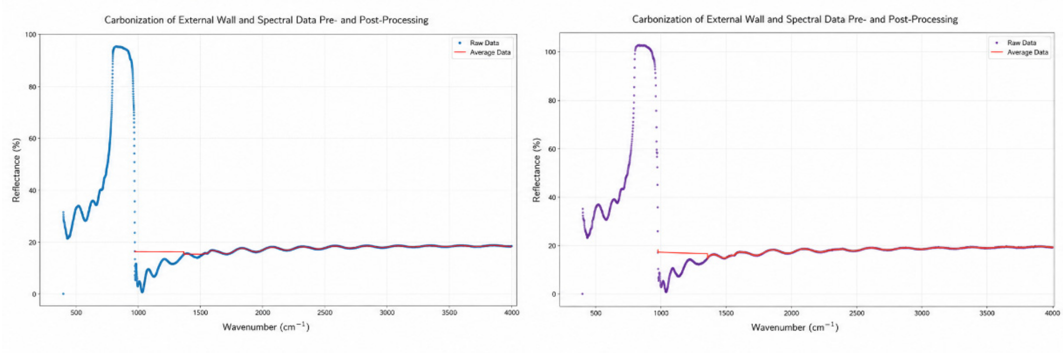

Figure 1. Data preprocessing results

To further compare the data quality before and after processing, the signal-to-noise ratio and periodic consistency are used as evaluation indicators. The results are shown in Table 1.

Table 1. Comparison of core quality indicators

Indicator	10° Original Data	10° Processed Data	15° Original Data	15° Processed Data
Signal-to-noise ratio (dB)	51.72	52.45	51.20	53.11
Periodic consistency	0.2841	0.8118	0.3171	0.4800

As shown in Table 1, the signal-to-noise ratio of both spectral datasets increases after preprocessing. For the 15° data, the signal-to-noise ratio increases from 51.20 dB to 53.11 dB. Periodic consistency also improves, with a more obvious change observed for the 10° data, increasing from 0.2841 to 0.8118. Together with Figure 1, the results indicate that the filtering reduces local noise while largely preserving the interference fringe structure, providing a more stable data basis for subsequent extremum detection and thickness inversion.

3. Construction of the Two-Beam Interference Thickness Inversion Model

When only one reflection and one transmission at each of the upper and lower interfaces of the epitaxial layer are considered, two main reflected beams are formed at the air–epitaxial layer interface and the epitaxial layer–substrate interface [5]. Because their propagation paths are different, an optical path difference is generated between the two beams, which further produces a stable phase difference and causes the reflectance to vary periodically with wavelength. Based on this relation, information associated with the epitaxial layer thickness can be extracted from the extrema of the spectrum.

3.1. Optical Path Difference Calculation

Assume that the infrared light is incident on the surface of the epitaxial layer at an incidence angle θ, with a refraction angle θ_t inside the layer, and that the refractive index of the epitaxial layer is n. Taking the refractive index of air as approximately 1, Snell's law gives: $n\sin\theta_t = \sin\theta$.

Accordingly, $\cos\theta_t = \sqrt{1-\sin^2\theta/n^2}$.

After entering the epitaxial layer, the beam is reflected at the lower interface and returns to the upper surface, completing one round trip inside the layer. If the epitaxial layer thickness is d, the optical path difference corresponding to this propagation path is:

$$\delta_1 = \frac{2nd}{\cos\theta_t} = 2d\sqrt{n^2 - \sin^2\theta} \tag{3}$$

Interface reflection also introduces an additional phase change. When light is reflected from an optically less dense medium toward an optically denser medium, a phase shift of π occurs, which can be treated as an additional optical path difference of half a wavelength: $\delta_2 = \frac{\lambda}{2}$.

The two contributions together give the total optical path difference:

$$\delta = 2d\sqrt{n^2 - \sin^2\theta} + \frac{\lambda}{2} \tag{4}$$

3.2. Phase Difference and Interference Condition

The phase difference corresponding to the total optical path difference can be written as:

$$\phi = \frac{4\pi d\sqrt{n^2 - \sin^2\theta}}{\lambda} + \pi \tag{5}$$

When the two beams have the same frequency and their polarization directions contain a common component, a stable phase difference can produce observable interference. For thickness inversion, the main quantities of interest are the positions of the reflectance maxima and minima, since the wavelengths corresponding to these extrema directly contain the propagation phase information.

3.3. Total Reflectance Model

Let the amplitude of the incident light be A_0, and let the amplitude reflection coefficients at the air–epitaxial layer interface and the epitaxial layer–substrate interface be r_1 and r_2, respectively. The complex amplitudes of the two main reflected beams are expressed as: $A_1 = A_0 r_1$ and $A_2 = A_0 r_2 t_1 t_1' e^{i\phi}$, where t_1 and t_1' denote the transmission coefficients when the beam enters and leaves the epitaxial layer, respectively. When absorption in the medium is neglected, $t_1 t_1' \approx 1$ can be used as an approximation, and the total reflected amplitude becomes: $A_{\text{total}} = A_0\left(r_1 + r_2 e^{i\phi}\right)$.

The reflectance R is defined as the ratio of reflected intensity to incident intensity:

$$R = \frac{|A_{\text{total}}|^2}{|A_0|^2} \tag{6}$$

Expanding the expression gives:

$$R = r_1^2 + r_2^2 + 2r_1 r_2 \cos\phi \tag{7}$$

The periodic oscillation of the reflectance is mainly determined by the $\cos\phi$ term. Therefore, the peak and valley positions in the spectrum reflect the variation of phase with wavelength and can be used as characteristic quantities for thickness inversion.

The amplitude reflection coefficients at the two interfaces are determined by the refractive indices of the media and the incidence conditions. For light incident from a medium with refractive index n_a into a medium with refractive index n_b, the amplitude reflection coefficient is:

$$r = \frac{n_a\cos\theta_i - n_b\cos\theta_t}{n_a\cos\theta_i + n_b\cos\theta_t} \tag{8}$$

where θ_i and θ_t are the incidence angle and refraction angle, respectively. After r_1 and r_2 are calculated from the optical parameters of the two interfaces, the corresponding theoretical reflectance can be obtained.

3.4. Interference Extremum Condition

The reflectance extrema correspond to the main peaks and valleys in the spectrum. Differentiating R with respect to wavelength gives:

$$\frac{dR}{d\lambda} = -2r_1r_2\sin\phi\frac{d\phi}{d\lambda} \tag{9}$$

When the reflectance reaches a local extremum: $\frac{dR}{d\lambda} = 0$.

Under the condition $\frac{d\phi}{d\lambda} \neq 0$ and $\sin\phi = 0$, that is, $\phi = k\pi, \quad k \in \mathbb{Z}$.

When $\phi = 2k\pi$, the two reflected beams are in phase and interfere constructively, corresponding to a reflectance maximum. When $\phi = (2k+1)\pi$, the two beams are out of phase and interfere destructively, corresponding to a reflectance minimum. Substituting the phase-difference expression gives:

$$\frac{4\pi d\sqrt{n^2 - \sin^2\theta}}{\lambda_k} + \pi = k\pi \tag{10}$$

which can be rearranged as $\frac{4d\sqrt{n^2 - \sin^2\theta}}{\lambda_k} = k - 1$.

A direct relation is therefore established among the interference order, the extremum wavelength, and the epitaxial layer thickness.

3.5. Thickness Calculation

A broadband infrared spectrum is used in the experiment. Different wavelength components experience different phase delays after propagating through the epitaxial layer, so the reflectance shows continuous oscillations with wavenumber. Compared with directly determining the absolute interference order of a single extremum, using the order difference between two extrema is more convenient for calculation and also eliminates the constant term [6].

Assume that two extrema correspond to wavelengths λ_m and λ_n, with interference orders m and n, respectively. Then:

$$\frac{4d\sqrt{n^2 - \sin^2\theta}}{\lambda_m} = m - 1, \quad \frac{4d\sqrt{n^2 - \sin^2\theta}}{\lambda_n} = n - 1 \tag{11}$$

Subtracting the two equations gives:

$$4d\sqrt{n^2 - \sin^2\theta}\left(\frac{1}{\lambda_m} - \frac{1}{\lambda_n}\right) = m - n \tag{12}$$

The epitaxial layer thickness can therefore be expressed as:

$$d = \frac{m - n}{4\sqrt{n^2 - \sin^2\theta}\left(\frac{1}{\lambda_m} - \frac{1}{\lambda_n}\right)} \tag{13}$$

This relation gives the thickness calculation under the two-beam interference condition. However, the refractive index n of an actual material varies with wavelength. If a fixed value is used over the entire spectral range, the calculated thickness may contain a systematic deviation. For this reason, the Cauchy dispersion model is introduced to describe the wavelength dependence of the refractive index and is incorporated into the subsequent iterative calculation.

4. Cauchy-Dispersion-Driven Joint Thickness Optimization Framework

The two-beam interference model gives the relationship between spectral extrema and the epitaxial layer thickness. However, the refractive index of an actual material is not constant and varies with wavelength. If a fixed refractive index is used directly, the dispersion characteristics in different wavelength ranges are ignored, which may affect the thickness estimation. Therefore, the Cauchy dispersion model is introduced to describe the wavelength dependence of the refractive index. Combined with extremum detection and iterative calculation, the refractive index parameters and epitaxial layer thickness are estimated together.

1. Extremum Detection

The thickness calculation depends on the periodically distributed peak and valley positions in the reflectance spectrum. After Savitzky–Golay filtering, local neighborhood comparisons are performed on the reflectance sequence. For the i th sampling point, when $R_i > R_{i-1}$, $R_i > R_{i+1}$ is satisfied, the point is identified as a local maximum. When $R_i < R_{i-1}$, $R_i < R_{i+1}$ is satisfied, it is identified as a local minimum. The detection results are shown in Figure 2.

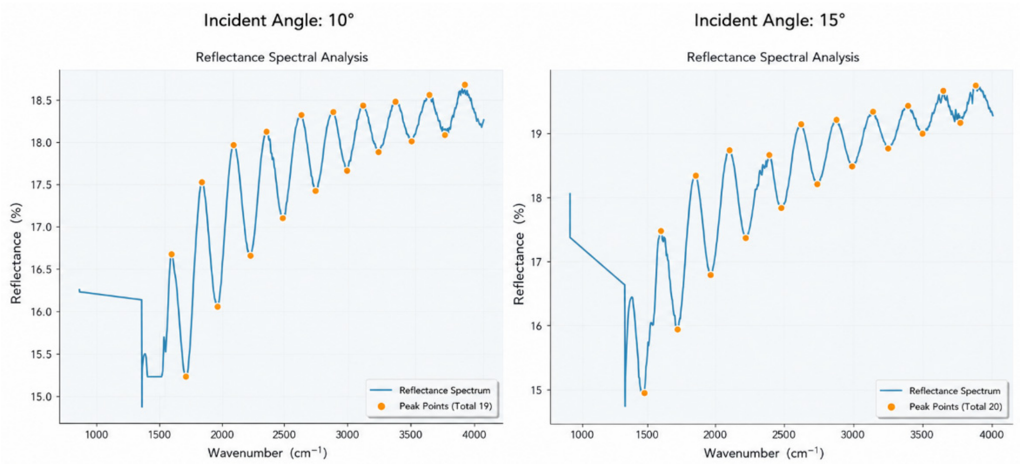

Figure 2. Reflectance spectrum at an incidence angle of 10° and 15°

The reflectance spectra at both incidence angles show clear periodic oscillations. A total of 19 valid extrema are detected under the 10° condition, while 20 are detected under the 15° condition. A small amount of local fluctuation remains in the high-wavenumber region, but the main peak and valley positions remain stable and have little effect on extremum identification. The detected extrema are then used for refractive index fitting and thickness calculation.

2. Cauchy Dispersion Model and Refractive Index Optimization

The SiC epitaxial layer shows noticeable dispersion within the wavelength range studied. A three-term Cauchy model is therefore used to describe the relationship between the refractive index n and wavelength λ:

$$n(\lambda) = A + \frac{B}{\lambda^2} + \frac{C}{\lambda^4} \tag{14}$$

where A, B, and C are the dispersion parameters to be estimated. Compared with a fixed refractive index, this model describes the variation in refractive index at different wavelengths and is more suitable for thickness inversion over a broad spectral range.

For the detected interference extrema, the refractive index at the corresponding wavelength can be derived from the interference condition. Let the interference order of an extremum be m. Then: $2nd\cos\theta' = m\lambda$.

Using Snell's law to eliminate the refraction angle θ' gives:

$$2d\sqrt{n^2 - \sin^2\theta} = m\lambda \tag{15}$$

The corresponding refractive index can then be written as:

$$n = \sqrt{\left(\frac{m\lambda}{2d}\right)^2 + \sin^2\theta} \tag{16}$$

At each iteration, the refractive index corresponding to each extremum is recalculated using the current thickness d, and the Cauchy model is then fitted to these values. Parameter estimation is performed using nonlinear least squares. The parameters A, B, C, and the thickness are updated by reducing the residual between the values calculated from the physical model and those predicted by the Cauchy model.

The initial thickness is set to $d = 10.0,\mu\mathrm{m}$, and the initial Cauchy parameters are set to $A = 2.6$, $B = 0.01$, and $C = 0.0001$. The parameter search ranges are set to $A \in [2.3, 3.0]$, $B \in [0.003, 0.03]$, and $C \in [0, 0.003]$, respectively. Since the thickness and refractive index are coupled, direct parameter updates may cause local oscillations. A damping factor is therefore included in the iterative process. The initial damping factor is set to 0.05. After every 10 iterations, if its value is below 0.5, the damping factor is increased to 1.1 times its previous value, allowing a balance between update stability and convergence speed.

3. Iterative Convergence and Thickness Calculation

The thickness iteration considers parameter changes, fitting error, and iteration status at the same time. When the relative change in thickness between two consecutive calculations is less than 0.1% and the fitting residual of the Cauchy model reaches the specified range, the parameters are considered to be basically stable. If the residual does not improve for 5 consecutive iterations, the current calculation is terminated to avoid remaining in a locally stable region for too long. The maximum number of iterations is set to 50, with a relative thickness change of less than 0.5% used as a safety termination condition.

After the optimized refractive index is obtained, multiple combinations of extrema are selected to recalculate the thickness. For the ith and jth extrema, the thickness is expressed as:

$$d_{ij} = \frac{|i-j| \times 10^4}{2\sqrt{n^2 - \sin^2\theta}, |\sigma_i - \sigma_j|} \tag{17}$$

where σ_i and σ_j are the wavenumbers of the corresponding extrema. During the calculation, $|i-j| \le 3$ is imposed to avoid additional effects caused by refractive index variation when the extrema are too far apart. The thickness values obtained from all valid combinations are then evaluated statistically, and their median is taken as the final estimate: $d = \mathrm{median}(d_{ij})$.

This treatment reduces the influence of positioning errors from individual extrema and makes the final thickness result more stable.

The variation in thickness with the number of iterations is shown in Figure 3.

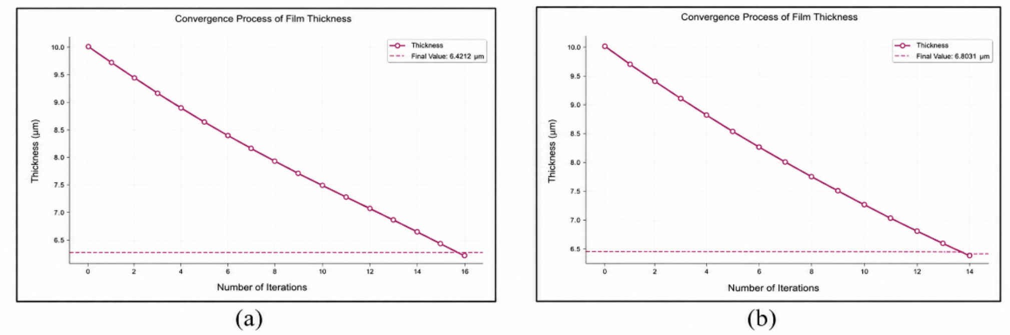

Figure 3. Convergence process of film thickness

At an incidence angle of 10°, the thickness stabilizes at 6.4212 μm after 16 iterations. Under the 15° condition, a thickness of 6.8031 μm is obtained after 14 iterations. Some stages of the iteration do not show a strictly monotonic change, which is related to the residual stagnation condition and damping updates. When the residual fails to decrease for several consecutive iterations, the calculation is terminated early rather than continuing with ineffective iterations. Both sets of results enter a stable range within a limited number of iterations, indicating that the iterative strategy can provide stable updates of the thickness parameter.

The estimated Cauchy model parameters and calculated thicknesses are shown in Table 2.

Table 2. Analysis results

Indicator	10°	15°
Film thickness	6.4212 μm	6.8031 $\pm$ 0.1 μm
A	2.596852	2.589647
B	0.015125 μm^2	0.007992 μm^2
C	0.00106592 μm^4	0.00022947 μm^4
RMSE	0.105395	0.076569
Number of detected extrema	19	20
Number of iterations	16	14

4. Cauchy Model Fitting Results

To examine how well the Cauchy model describes the variation in refractive index, the refractive indices obtained from the extrema at both incidence angles are fitted over the full spectral range. The results are shown in Figure 4.

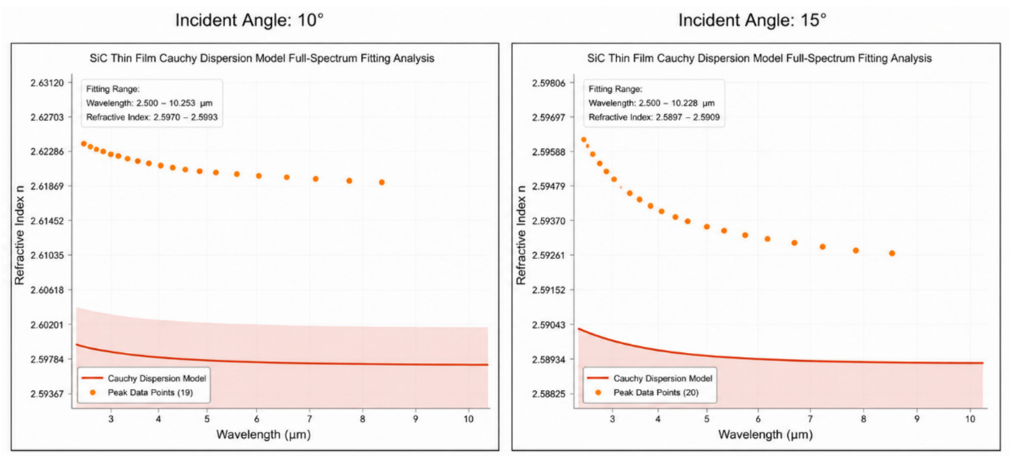

Figure 4. Full-spectrum fitting analysis at an incidence angle of 10° and 15°

ISSN: 2688-8645

The fitted wavelength range at angle of 10° is approximately 2.500–10.253 μm, with the refractive index mainly distributed between 2.5970 and 2.5993. At angle of 15°, the wavelength range is approximately 2.500–10.228 μm, and the refractive index is approximately 2.5897–2.5909. The refractive index varies relatively slowly in both datasets, although the fitting performance differs between them.

Under the 15° condition, the extrema-derived refractive index values are generally closer to the Cauchy fitting curve, which is consistent with the RMSE results in Table 2. The corresponding RMSE decreases from 0.105395 at 10° to 0.076569 at 15°, indicating that the 15° data agree better with the current dispersion model. At the same time, there is still a difference between the thicknesses obtained under the two incidence conditions. This suggests that, in addition to material dispersion, multiple reflections of light inside the epitaxial layer may also affect the thickness inversion. It is therefore necessary to further analyze the multiple-beam interference condition.

5. Multiple-Beam Interference Identification and Thickness Correction Model

5.1. Multiple-Beam Interference Conditions

The two-beam model only considers the two main reflected beams from the upper and lower interfaces of the epitaxial layer. When the interface reflection is relatively strong, part of the light undergoes multiple reflections and transmissions inside the epitaxial layer, forming several reflected beams with fixed phase relationships. In this case, higher-order reflected beams also contribute to the total light intensity, and the two-beam approximation may no longer be sufficient to describe the actual interference process. It is therefore necessary to determine whether multiple-beam interference is present.

The multiple-beam effect is first influenced by the reflectivity of the interfaces. Let the reflectivities of the two interfaces be R_1 and R_2. When $R_1 R_2 > 0.01$ is satisfied, the higher-order reflected beams do not decay rapidly after only a few reflections, and their contribution to the final reflectance spectrum cannot be neglected.

In addition to reflectivity, the beams must also maintain sufficient coherence. Let the central wavelength of the light source be λ, and let the effective spectral bandwidth be $\Delta\lambda$. The coherence length can then be approximated as: $L_c \approx \frac{\lambda^2}{\Delta\lambda}$.

The optical path difference between adjacent reflected beams is $\Delta L = 2nd\cos\theta$.

When $2nd\cos\theta < L_c$ is satisfied, the beams after multiple reflections can still maintain stable interference. By combining the reflectivity condition and the coherence-length condition, it can be determined whether higher-order reflected beams need to be included in the thickness calculation model.

5.2. Multiple-Beam Interference Thickness Model

Under multiple-beam interference conditions, continuous reflections and transmissions at the upper and lower interfaces of the epitaxial layer produce a series of reflected components with fixed phase differences. Therefore, the total reflected amplitude should be expressed as the superposition of reflected beams of different orders: $A_{\text{total}} = A_1 + A_2 + A_3 + \cdots$.

Let the amplitude reflection coefficient of the air–epitaxial layer interface be r_1, the amplitude reflection coefficient of the epitaxial layer–substrate interface be r_2, and the phase difference between adjacent reflected beams be ϕ. The total reflected amplitude can then be expressed as:

$$A_{\text{total}} = A_0\left[r_1 + t_1 t_1' r_2 e^{i\phi}\left(1 + r_1 r_2 e^{i\phi} + (r_1 r_2 e^{i\phi})^2 + \cdots\right)\right] \tag{18}$$

When $|r_1 r_2| < 1$, the above series converges. After neglecting absorption in the medium, the reflectance under multiple-beam interference can be expressed as:

$$R = \frac{F\sin^2(\phi/2)}{1 + F\sin^2(\phi/2)} \tag{19}$$

where $F = \dfrac{4R_{\text{eff}}}{(1-R_{\text{eff}})^2}$ and R_{eff} is the effective reflection coefficient formed by the two interfaces.

Multiple-beam interference does not change the basic relationship between optical path difference and thickness, but the reflectance expression and the corresponding extremum conditions are different. When the reflectance reaches a minimum, $\phi = 2k\pi$,which gives

$$\frac{4d\sqrt{n^2 - \sin^2\theta}}{\lambda_k} = 2k - 1 \tag{20}$$

For two adjacent minima,

$$\frac{4d\sqrt{n^2 - \sin^2\theta}}{\lambda_{k+1}} = 2k + 1 \tag{21}$$

Subtracting the two equations gives:

$$4d\sqrt{n^2 - \sin^2\theta}\left(\frac{1}{\lambda_k} - \frac{1}{\lambda_{k+1}}\right) = 2 \tag{22}$$

Therefore, the thickness under multiple-beam interference can be expressed as:

$$d = \frac{1}{2\sqrt{n^2 - \sin^2\theta}\left(\dfrac{1}{\lambda_k} - \dfrac{1}{\lambda_{k+1}}\right)} \tag{23}$$

Using the wavenumber $\sigma = 1/\lambda$, the expression can be further written as:

$$d = \frac{1}{2\sqrt{n^2 - \sin^2\theta}\left(\sigma_k - \sigma_{k+1}\right)} \tag{24}$$

The main differences between the two-beam and multiple-beam models are shown in Table 3.

Table 3. Comparison of two-beam and multiple-beam interference models

Feature	Two-Beam Interference	Multiple-Beam Interference
Reflectance model	$R = r_1^2 + r_2^2 + 2r_1 r_2\cos\phi$	$R = \dfrac{F\sin^2(\phi/2)}{1 + F\sin^2(\phi/2)}$
Minimum condition	$\phi = (2k+1)\pi$	$\phi = 2k\pi$
Thickness relation	$d = \dfrac{1}{4\sqrt{n^2 - \sin^2\theta}\left(\sigma_k - \sigma_{k+1}\right)}$	$d = \dfrac{1}{2\sqrt{n^2 - \sin^2\theta}\left(\sigma_k - \sigma_{k+1}\right)}$

Table 3 shows that the main differences between the two models lie in the reflectance expression, the extremum condition, and the thickness calculation relation. When higher-order reflected beams participate in the interference, continuing to use the two-beam model may introduce a certain thickness calculation error. In such cases, the multiple-beam model is needed for correction.

5.3. Multiple-Beam Interference Determination and Thickness Calculation

Based on the reflectivity threshold and coherence-length criteria, multiple-beam interference is examined for the spectra measured at different incidence angles. The reflectivities of the two interfaces are first calculated to determine whether $R_1 R_2 > 0.01$ is satisfied.

The optical path difference between adjacent reflected beams is then calculated as $\Delta L = 2nd\cos\theta$ and compared with the effective coherence length L_c.

The calculation results show that both sets of measurement data satisfy the interface reflectivity and coherence-length criteria. The effect of higher-order reflected beams on the reflectance spectra therefore cannot be neglected, and the multiple-beam model is used for thickness calculation.

During the calculation, the Cauchy dispersion model and the refractive index fitting procedure are retained, while only the thickness relation is replaced by:

$$d = \frac{1}{2\sqrt{n^2 - \sin^2\theta}\left(\sigma_k - \sigma_{k+1}\right)} \tag{25}$$

This keeps the refractive index fitting procedure consistent and avoids rebuilding a separate parameter estimation model.

5.4. Correction of Multiple-Beam Interference Effects

When higher-order reflected beams participate in the interference, the peak and valley positions in the reflectance spectrum may shift to some extent, and the thickness obtained from the two-beam model may also contain a corresponding deviation. Since the interface reflectivity is mainly determined by the material itself, the multiple-beam coherence effect is reduced by adjusting the optical path difference.

During the calculation, the equivalent propagation distance is increased so that the optical path difference between adjacent reflected beams gradually becomes larger. When $\Delta L = 2nd\cos\theta \geq L_c$ is satisfied, the higher-order reflected beams can no longer maintain a stable phase relationship easily, and their contribution to the reflectance spectrum is reduced. The refractive index fitting and thickness iteration are then performed again. The corrected calculation results are shown in Table 4.

Table 4. Calculation results after correction of multiple-beam interference effects

Indicator	10°	15°
Film thickness (μm)	8.463	8.532
Cauchy parameter A	2.7889	2.8221
Cauchy parameter B (μm^2)	0.005816	0.004897
Cauchy parameter C (μm^4)	0.00003662	0.00004262
Fitting error RMSE	0.099427	0.11039
Number of detected extrema	19	20
Number of iterations	22	24

After correction, the thicknesses corresponding to the two incidence angles are 8.463 μm and 8.532 μm, respectively, showing good consistency. Although there are some differences in the Cauchy parameters and RMSE values between the two datasets, the final thickness results are relatively close, indicating that the multiple-beam model can maintain stable thickness estimation under different incidence angles.

Compared with the two-beam model, the corrected thickness results change noticeably, indicating that higher-order reflected beams have a certain influence on thickness inversion. For measurement data that satisfy the multiple-beam interference conditions, determining the appropriate interference model before thickness calculation can reduce the effect of model selection on the estimated thickness and improve the consistency of the results obtained at different incidence angles.

6. Conclusion

This paper focuses on the inversion of epitaxial layer thickness using infrared reflectance spectroscopy and establishes a computational framework that integrates spectral filtering, dispersion parameter optimization, and interference mode correction. Experimental results show that the Cauchy dispersion model can effectively describe refractive index variations across a wide spectral range, and when combined with damped iteration, it enables stable convergence of the thickness parameters; After further accounting for higher-order reflections and applying corrections based on a multi-beam interference model, the thicknesses under 10° and 15° incidence were determined to be 8.463 μm and 8.532 μm, respectively. Compared to the 6.4212 μm and 6.8031 μm obtained using the two-beam model, the consistency of the results across different incidence angles was significantly improved. The study demonstrates that joint modeling of dispersion characteristics and interference modes can reduce the impact of model selection on thickness inversion, providing a reliable method for calculating epitaxial layer thickness under various measurement conditions. Future research could further enhance the model's adaptability to complex optical conditions.

References

[1] Shi, S. Z., Ma, L. Y., Wang, Z. Y., et al. (2022). Preparation of amorphous aluminum oxide thin films by atomic layer deposition and their spectral ellipsometry. Micro-Nano Electronics Technology, 59(11), 1218–1225+1241. https://doi.org/10.13250/j.cnki.wndz.2022.11.016.

[2] Du, L. M., Guan, Y. Q., Kong, M., et al. (2021). Thickness measurement and traceability of nanothin films based on Müller ellipsometry. Micro-Nano Electronics Technology, 58(12), 1121–1127. https://doi.org/10.13250/j.cnki.wndz.2021.12.012.

[3] Wang, C. Q., Sun, J. Y., Chen, Y. J., et al. (2026). Study on an infrared interferometric thickness measurement model based on dispersion correction and full-spectrum fitting. Mathematical Modeling and Its Applications, 15(1), 104–113. https://doi.org/10. 19943/j. 2095-3070. jmmia. 2026. 01.11.

[4] Dong, S., Long, Z. Y., Bi, J. F., et al. (2023). A method for analyzing bridge structural monitoring data based on Savitzky–Golay smoothing and wavelet denoising. Surveying and Mapping Bulletin, (9), 100–106. https://doi.org/10.13474/j.cnki.11-2246.2023.0272.

[5] Yang, L., Chen, S. Q., Xu, Y. Y., et al. (2026). A study on the thickness measurement of epitaxial layers using dual-beam and multi-beam infrared interferometry. Journal of Southwest Minzu University (Natural Science Edition). https://link.cnki.net/urlid/51.1672.N.20260716.1013.002.

[6] Zhang, X. C., Xu, W. N., Zhou, S. H. (2026). Modeling and analysis of epitaxial layer thickness measurement using infrared interferometry. Mathematical Modeling and Its Applications, 15(1), 86–93. https://doi.org/10.19943/j.2095-3070.jmmia.2026.01.09.